

Supplementary Information

Effect of Ion to Ligand Ratio on the Aqueous to Organic Relative Solubility of a Lanthanide-Ligand Complex

Thomas J. Summers,^{1,#} Jesus Diaz Sanchez,¹ David C. Cantu^{1,*}

¹*Department of Chemical and Materials Engineering, University of Nevada, Reno, Reno, NV,
USA*

*Corresponding author: dcantu@unr.edu

#Present address: Los Alamos National Laboratory, Los Alamos, NM, USA

Table S1. Details on model construction.

Exchanged Molecule	Water Molecule Count	Organic Molecule Count	Additional Components	Equilibrated Box Dimensions (nm)
Ethylbenzene	3500	500 octanol	--	$4.17752 \times 4.17752 \times 13.61871$
	3500	500 hexane	--	$4.07038 \times 4.07038 \times 13.02523$
Formamide	3500	500 octanol	--	$4.17803 \times 4.17803 \times 13.62040$
	3500	500 hexane	--	$4.07259 \times 4.07259 \times 13.03228$
Acetonitrile	3500	500 octanol	--	$4.17581 \times 4.17581 \times 13.61316$
	3500	500 hexane	--	$4.08276 \times 4.08276 \times 13.06482$
Gd ³⁺	3500	500 octanol	3 Cl ⁻	$4.17535 \times 4.17535 \times 13.61165$
	3500	500 hexane	3 Cl ⁻	$4.44776 \times 4.44776 \times 10.94147$
HDEHP	4000	500 octanol	1 Na ⁺	$4.25623 \times 4.25623 \times 14.00299$
	4000	500 hexane	1 Na ⁺	$4.13736 \times 4.13736 \times 13.61191$
Gd(HDEHP)	4000	500 octanol	2 Cl ⁻	$4.24756 \times 4.24756 \times 13.97450$
	4000	500 hexane	2 Cl ⁻	$4.14806 \times 4.14806 \times 13.64711$
Gd(HDEHP) ₂	4850	575 octanol	1 Cl ⁻	$4.39440 \times 4.29440 \times 15.38038$
	4850	775 hexane	1 Cl ⁻	$4.50606 \times 4.50606 \times 15.77123$
Gd(HDEHP) ₃	4850	575 octanol	--	$4.40599 \times 4.40599 \times 15.42095$
	4850	775 hexane	--	$4.50933 \times 4.50933 \times 15.78266$

DEHP⁻ gromacs topology file appears at the end of the SI

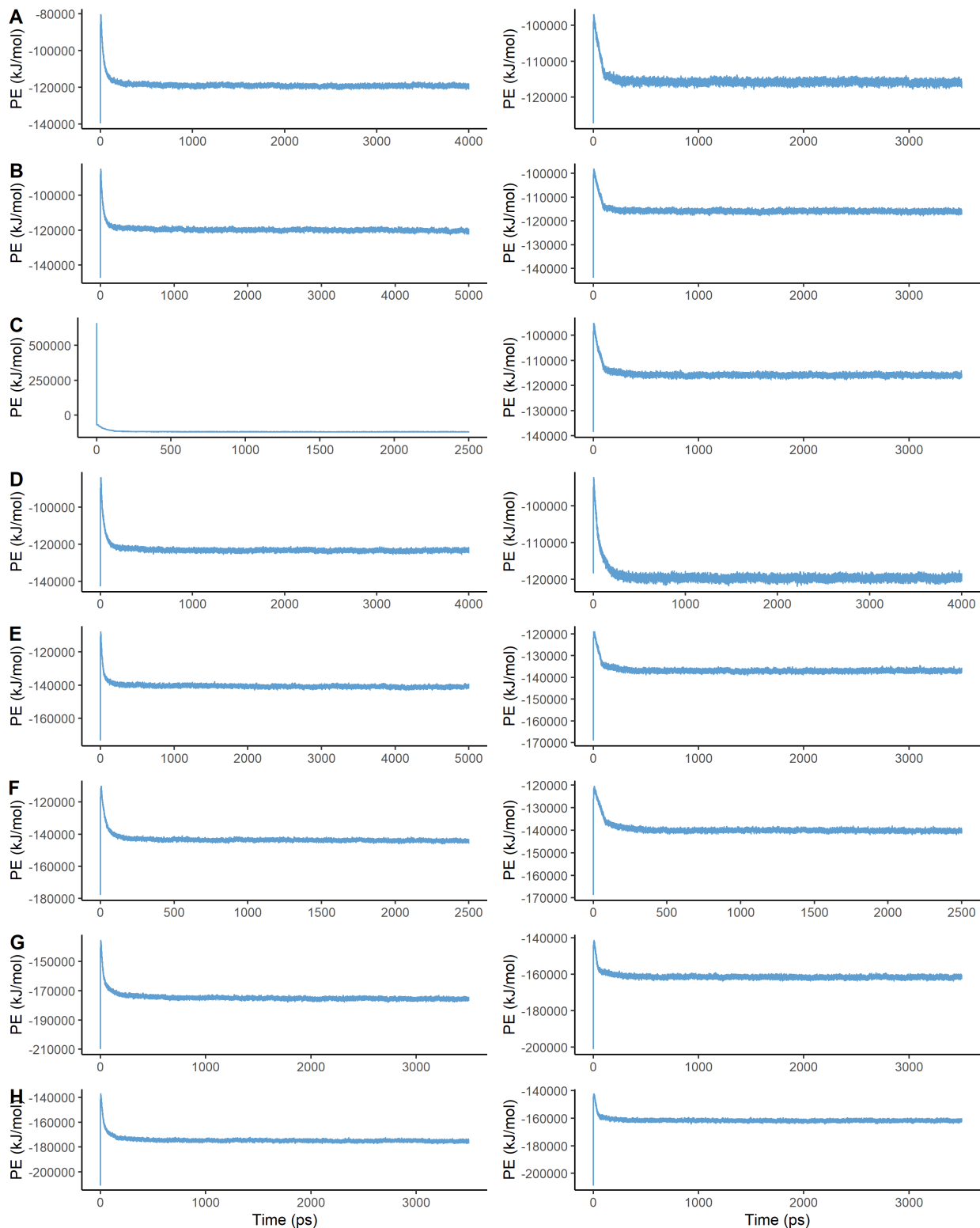


Figure S1. Plots of the potential energy (PE) of the biphasic system equilibrations of water and either octanol (left column) or hexane (right column) for the simulations of (A) ethylbenzene, (B) formamide, (C) acetonitrile, (D) Gd^{3+} ion, (E) DEHP^- ion, (F) Gd-DEHP 1:1, (G) Gd-DEHP 1:2, and (H) Gd-DEHP 1:3.

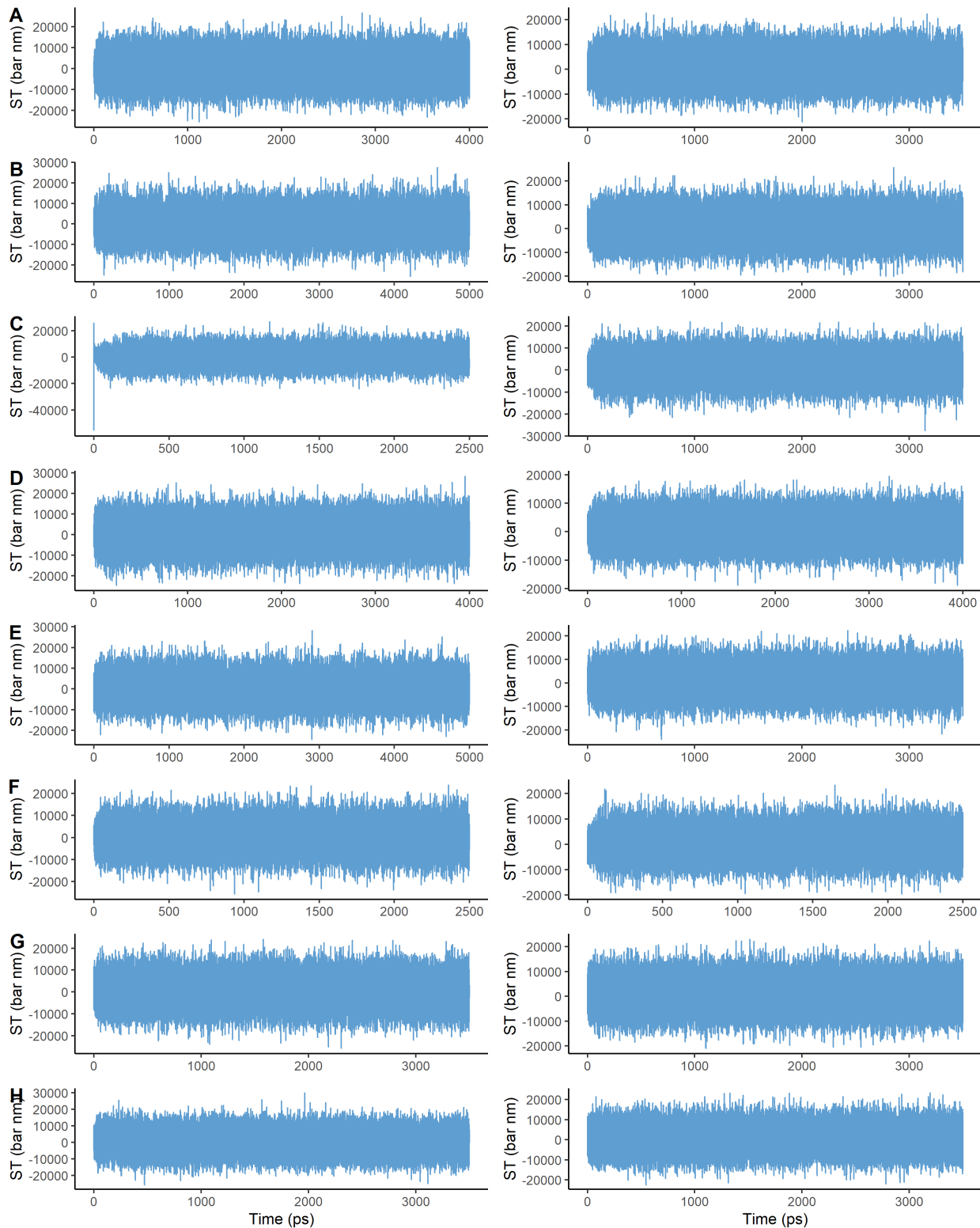


Figure S2. Plots of the surface tension of the biphasic system equilibrations of water and either octanol (left column) or hexane (right column) for the simulations of (A) ethylbenzene, (B) formamide, (C) acetonitrile, (D) Gd^{3+} ion, (E) DEHP^- ion, (F) Gd-DEHP 1:1, (G) Gd-DEHP 1:2, and (H) Gd-DEHP 1:3.

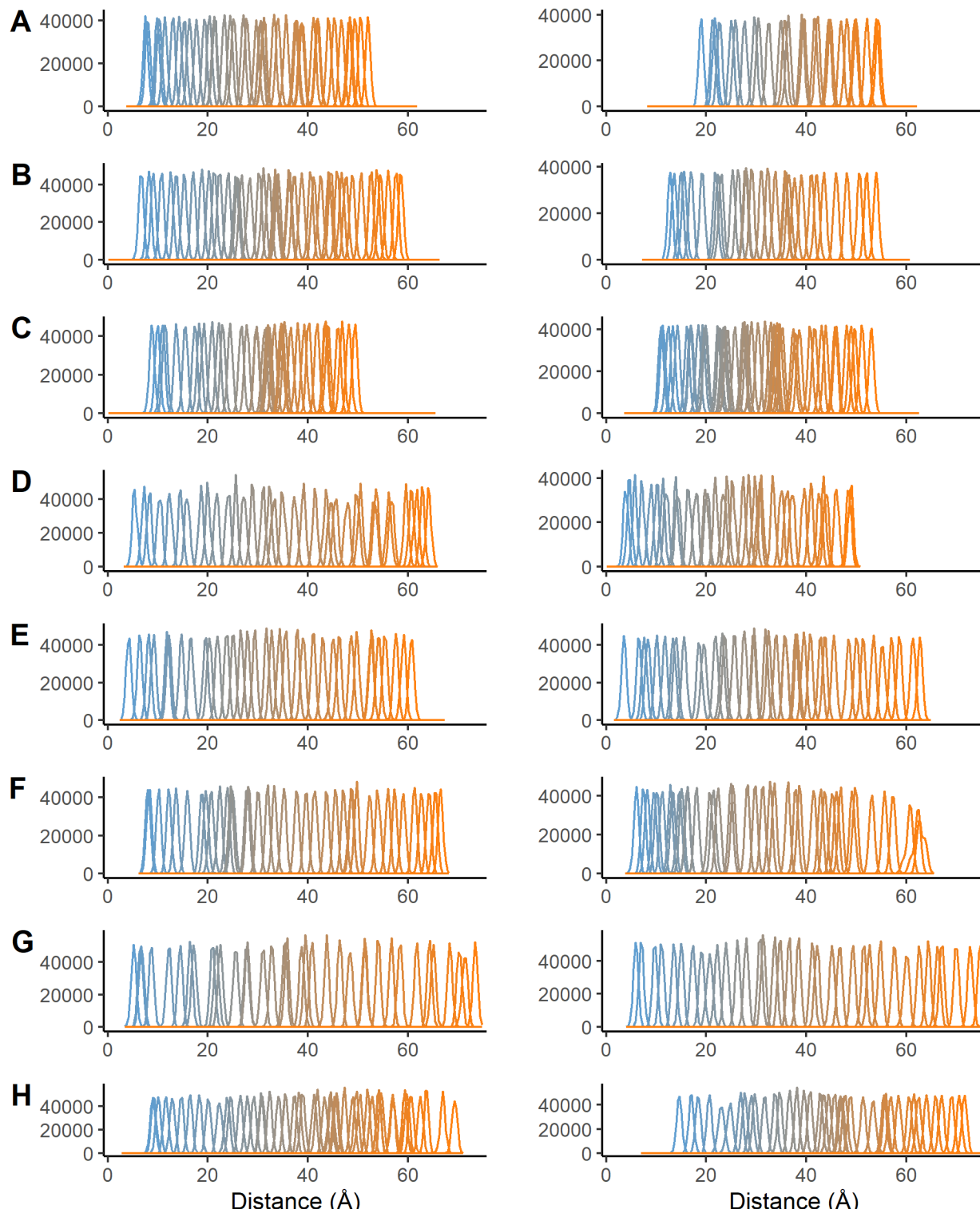


Figure S3. Umbrella sampling windows (Y-axis is sampling count) as the molecules transfer from water to either octanol (left column) or hexane (right column) for (A) ethylbenzene, (B) formamide, (C) acetonitrile, (D) Gd^{3+} ion, (E) DEHP^- ion, (F) Gd-DEHP 1:1, (G) Gd-DEHP 1:2, and (H) Gd-DEHP 1:3.

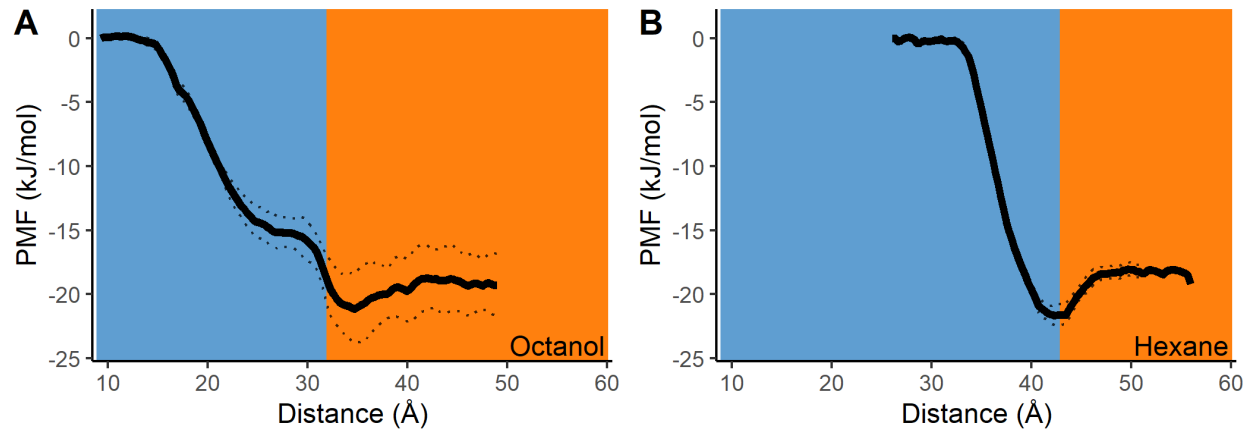


Figure S4. The potential of mean force as an ethylbenzene molecule transfers from bulk water into (A) octanol or (B) hexane. Background coloring indicates the transition from contact with bulk water (blue) to a mixture (light orange) and to bulk organic (dark orange). Dotted lines indicate statistical upper and lower bounds of the PMF.

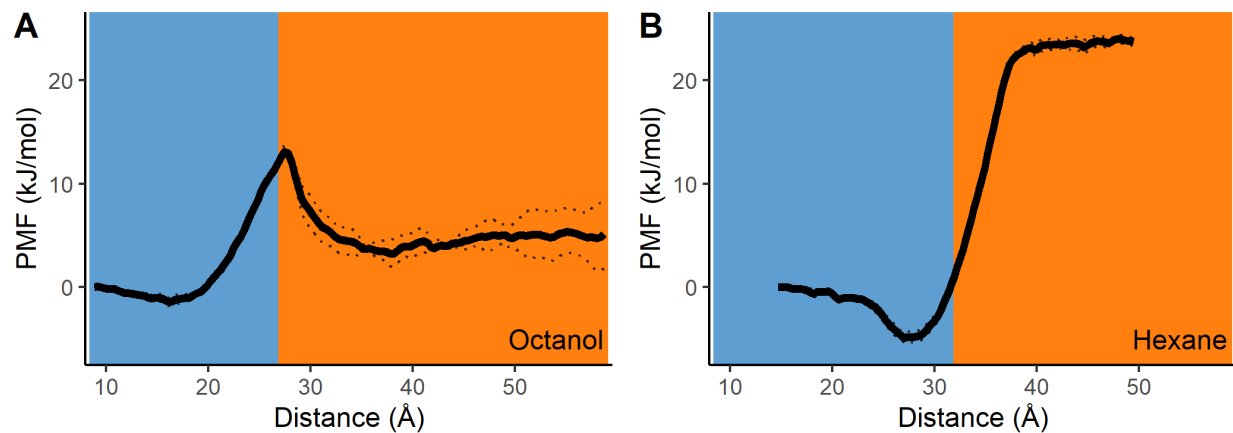


Figure S5. The potential of mean force as a formamide molecule transfers from bulk water into (A) octanol or (B) hexane. Background coloring is same as in Figure S1. Dotted lines indicate statistical upper and lower bounds of the PMF.

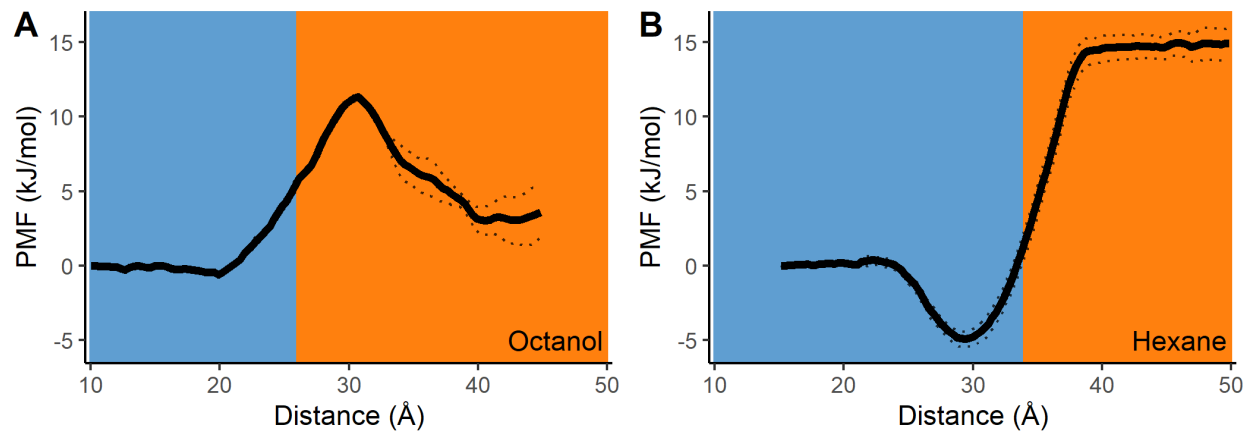


Figure S6. The potential of mean force as an acetonitrile molecule transfers from bulk water into (A) octanol or (B) hexane. Background coloring is same as in Figure S1. Dotted lines indicate statistical upper and lower bounds of the PMF.

Supplementary information on the unbound Gd^{3+} ion simulations

As the Gd^{3+} ion enters octanol (Figure S7A), the free energy rapidly increases monotonically with no plateauing observed over the length of the simulation. The absence of a plateau in the bulk octanol arises from the limited size of the simulation box and due to the formation of a water finger as the Gd^{3+} hydration complex brings along additional water molecules with it into the organic phase (Figure S7C). As the ion progressed deeper into the bulk octanol, the water finger continued extending and remained intact over the distance covered in this simulation. A water finger also formed when the ion enters the bulk hexane. However, as hexane lacks the hydrophilic head groups of octanol, the volume of the water entering the bulk hexane layer is much greater and thermodynamically more unfavorable (Figure S7B). The observation of water finger formations follows trends seen in previous studies on ion transfer from water into an immiscible liquid.*

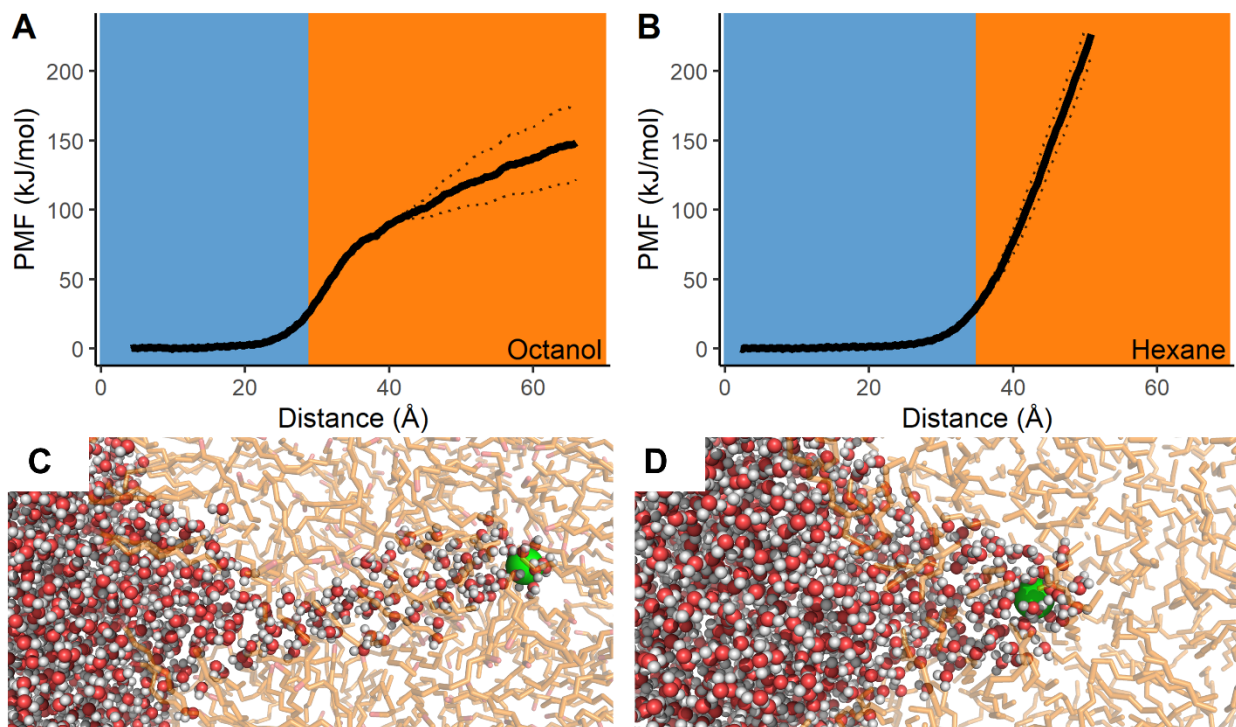


Figure S7. (A, B) Potential of mean force as a Gd^{3+} ion transfers from aqueous to either octanol or hexane layers. Dotted lines indicate statistical upper and lower bounds of the PMF. (C) Water tunnel formed as Gd^{3+} enters bulk octanol. (D) Water tunnel formed as Gd^{3+} enters bulk hexane. Coloring is same as Figure 1 with Gd^{3+} ion shown as a green sphere.

* (1) Ilan Benjamin, *Science*, 1993, **261**, 1558–1560. (2) A. Morita, A. Koizumi and T. Hirano, *J. Chem. Phys.*, 2021, **154**, 080901. (3) N. Kikkawa, L. Wang and A. Morita, *J. Am. Chem. Soc.*, 2015, **137**, 8022–8025. (4) J. J. Karnes and I. Benjamin, *J. Chem. Phys.*, 2016, **145**, 014701.

Supplementary information on the unrestrained DEHP⁻ ion simulations

As additional verification that the DEHP⁻ molecule does readily incorporate into the water-organic interfaces, we conducted additional simulations following the same methodology where an equilibrated system containing the DEHP⁻ molecule positioned within either bulk aqueous or bulk organic layers was simulated for 25ns without any constraints. While the DEHP⁻ molecule readily integrated into the interfacial layer when its starting position was within bulk water or within bulk hexane, it was not able to break past the ordered octanol tails at the octanol-water interface when it was within bulk octanol and so it remained in the octanol layer. This octanol-water simulation was extended to a total time of 200ns without any change; we anticipate that observation of this event without direction would require additional simulation time, but this is beyond the intended purpose of these simulations. The results of the simulations can be quantified by the radial distribution of the DEHP⁻ molecule to nearby solvent molecules (Figure S8). The graphs illustrate the frequent contact between ligand to both water and hexane in the water-hexane simulations as it resides at the interface (Figure S8A) and water and octanol when the ligand begins within bulk water (Figure S8B, right), but there is only frequent contact with octanol molecules when the ligand is initially positioned in the bulk octanol layer (Figure S8B, left).

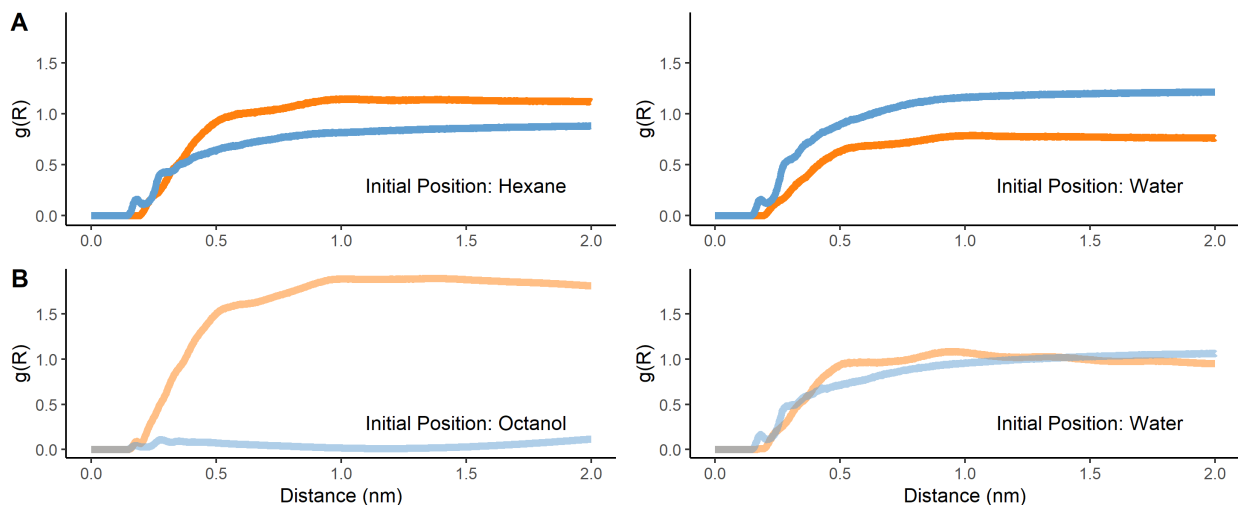


Figure S8. Radial distribution functions of the DEHP⁻ molecule to nearby water (blue) or organic molecules (orange) for (A) the hexane-water and (B) octanol-water systems when the DEHP⁻ molecule begins in bulk organic (left) or aqueous (right) phases.

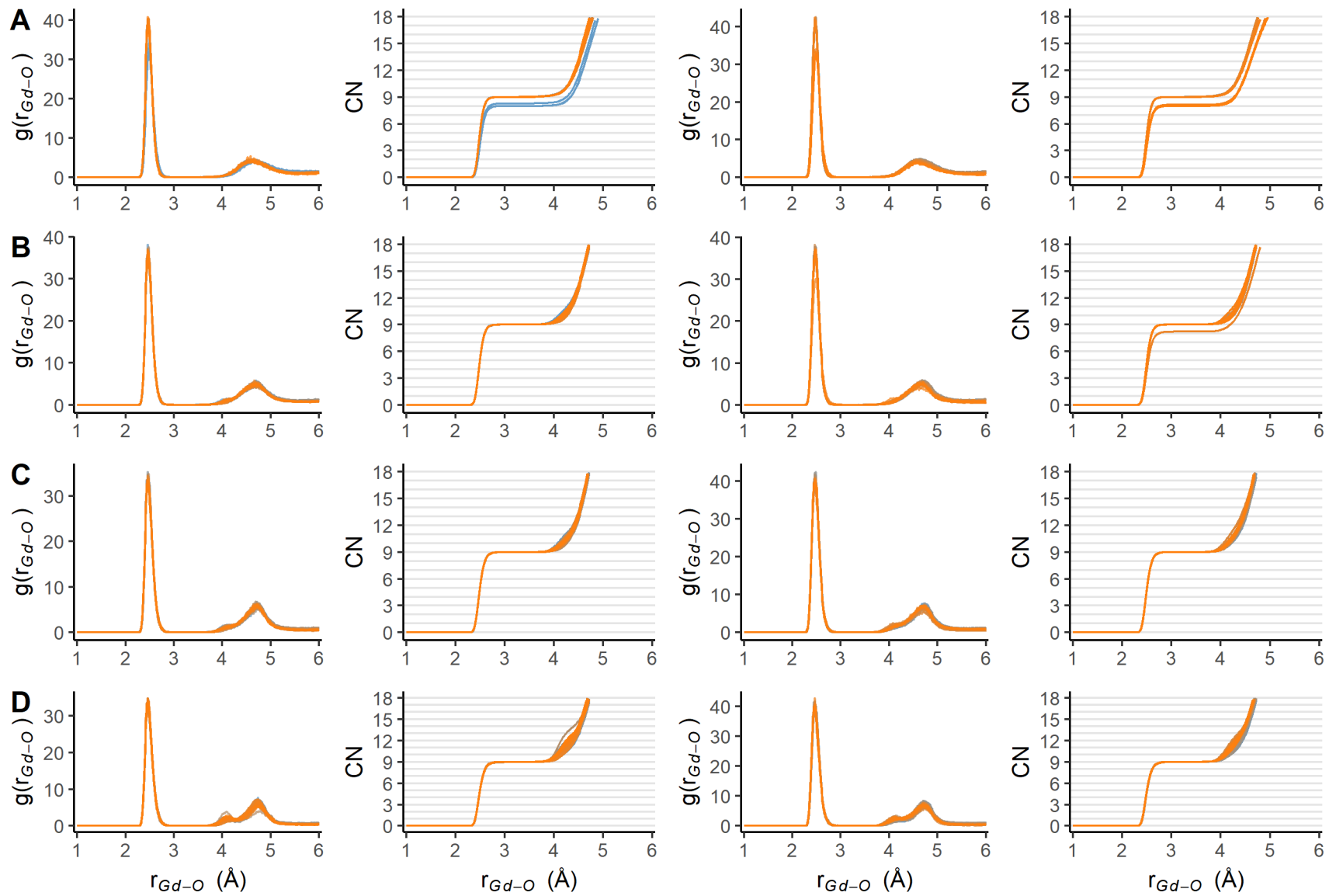


Figure S9. Plots of Gd-O radial distribution functions and coordination numbers (CN) from the umbrella simulations of the transfer of free Gd ion (A) and Gd-DEHP⁻ in 1:1 (B), 1:2 (C) and 1:3 (D) ratios from water to octanol (left columns) or hexane (right)

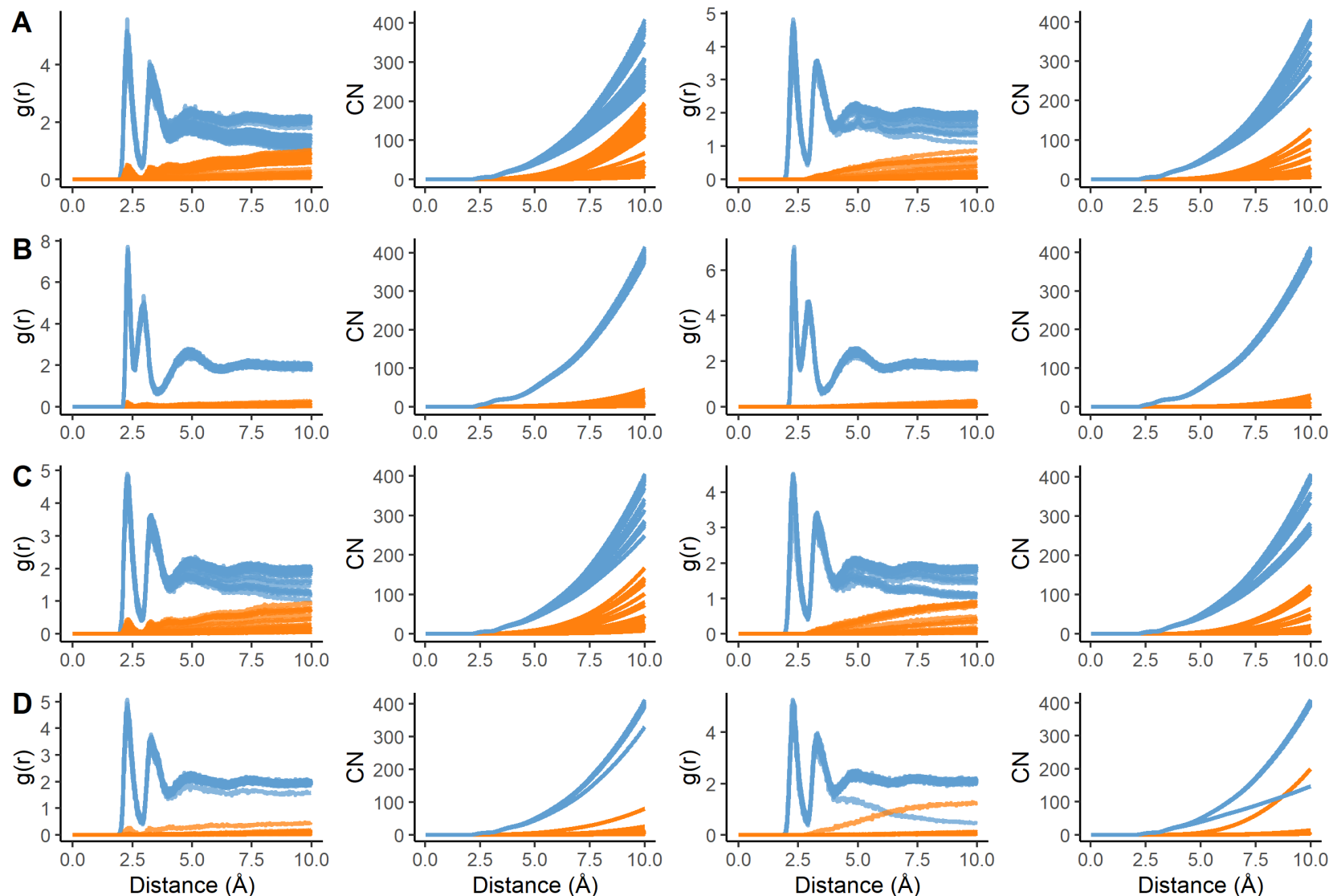


Figure S10. Radial distribution functions and coordination numbers (CN) for the counterions to the center of mass of water (blue) and organic (orange) molecules from the umbrella simulations of the transfer of free Gd ion (A), DEHP⁻ ion (B), and Gd-DEHP⁻ in 1:1 (C), and 1:2 (D) ratios with octanol (left columns) or hexane (right) as the organic solvent.

DEHP structure in GROMACS format

	Green	Red	Orange	Magenta	Azure	Cyan	Skyblue
55							
1HDE	01	1	0.037	0.206	-0.159		
1HDE	P1	2	-0.071	0.195	-0.264		
1HDE	O2	3	-0.182	0.093	-0.250		
1HDE	O3	4	-0.002	0.181	-0.414		
1HDE	O4	5	-0.132	0.346	-0.283		
1HDE	C1	6	0.054	0.054	-0.451		
1HDE	H1	7	0.147	0.038	-0.395		
1HDE	H2	8	-0.015	-0.026	-0.423		
1HDE	C2	9	-0.244	0.366	-0.372		
1HDE	H3	10	-0.218	0.327	-0.471		
1HDE	H4	11	-0.330	0.309	-0.336		
1HDE	C3	12	-0.278	0.515	-0.377		
1HDE	C4	13	-0.159	0.604	-0.422		
1HDE	C5	14	-0.411	0.539	-0.454		
1HDE	H5	15	-0.198	0.705	-0.440		
1HDE	H6	16	-0.091	0.613	-0.336		
1HDE	C6	17	-0.076	0.558	-0.542		
1HDE	H7	18	-0.437	0.645	-0.443		
1HDE	H8	19	-0.490	0.483	-0.402		
1HDE	C7	20	-0.415	0.502	-0.603		
1HDE	H9	21	-0.139	0.547	-0.631		
1HDE	H10	22	-0.032	0.460	-0.522		
1HDE	C8	23	0.038	0.656	-0.575		
1HDE	H11	24	-0.517	0.516	-0.642		
1HDE	H12	25	-0.349	0.565	-0.663		
1HDE	H13	26	-0.388	0.398	-0.621		
1HDE	H14	27	0.101	0.669	-0.485		
1HDE	H15	28	-0.004	0.755	-0.597		
1HDE	C9	29	0.126	0.610	-0.692		
1HDE	H16	30	0.067	0.600	-0.784		
1HDE	H17	31	0.206	0.682	-0.712		
1HDE	H18	32	0.172	0.513	-0.671		
1HDE	C10	33	0.083	0.053	-0.601		
1HDE	C11	34	0.168	-0.070	-0.641		
1HDE	C12	35	-0.043	0.076	-0.688		
1HDE	H19	36	0.199	-0.057	-0.746		
1HDE	H20	37	0.261	-0.067	-0.582		
1HDE	C13	38	0.106	-0.210	-0.625		
1HDE	H21	39	-0.017	0.054	-0.793		
1HDE	H22	40	-0.066	0.184	-0.686		
1HDE	C14	41	-0.171	0.000	-0.650		
1HDE	H23	42	0.020	-0.221	-0.693		
1HDE	H24	43	0.067	-0.223	-0.524		
1HDE	C15	44	0.206	-0.322	-0.655		
1HDE	H25	45	-0.252	0.025	-0.720		
1HDE	H26	46	-0.158	-0.108	-0.652		
1HDE	H27	47	-0.205	0.028	-0.549		
1HDE	H28	48	0.292	-0.313	-0.587		
1HDE	H29	49	0.246	-0.309	-0.757		
1HDE	C16	50	0.146	-0.463	-0.642		
1HDE	H30	51	0.062	-0.476	-0.711		
1HDE	H31	52	0.220	-0.540	-0.664		
1HDE	H32	53	0.108	-0.480	-0.541		
1HDE	H33	54	0.148	0.140	-0.620		
1HDE	H34	55	-0.300	0.544	-0.273		
	0.00000	0.00000	0.00000				

DEHP parameters

HDE 3

[atoms]

1	opls_441	1	HDE	O1	1	-0.867 15.999400
2	opls_440	1	HDE	P1	2	1.7108 30.973760
3	opls_441	1	HDE	O2	3	-0.867 15.999400
4	opls_442	1	HDE	O3	4	-0.8043 15.999400
5	opls_442	1	HDE	O4	5	-0.8043 15.999400
6	opls_443	1	HDE	C1	6	0.0546 12.011000
7	opls_444	1	HDE	H1	7	0.1623 1.008000
8	opls_444	1	HDE	H2	8	0.1623 1.008000
9	opls_443	1	HDE	C2	9	0.0546 12.011000
10	opls_444	1	HDE	H3	10	0.1623 1.008000
11	opls_444	1	HDE	H4	11	0.1623 1.008000
12	opls_137	1	HDE	C3	12	-0.1823 12.011000
13	opls_136	1	HDE	C4	13	-0.312 12.011000
14	opls_136	1	HDE	C5	14	-0.312 12.011000
15	opls_140	1	HDE	H5	15	0.1551 1.008000
16	opls_140	1	HDE	H6	16	0.1551 1.008000
17	opls_136	1	HDE	C6	17	-0.312 12.011000
18	opls_140	1	HDE	H7	18	0.1551 1.008000
19	opls_140	1	HDE	H8	19	0.1551 1.008000
20	opls_135	1	HDE	C7	20	-0.4965 12.011000
21	opls_140	1	HDE	H9	21	0.1551 1.008000
22	opls_140	1	HDE	H10	22	0.1551 1.008000
23	opls_136	1	HDE	C8	23	-0.312 12.011000
24	opls_140	1	HDE	H11	24	0.1591 1.008000
25	opls_140	1	HDE	H12	25	0.1591 1.008000
26	opls_140	1	HDE	H13	26	0.1591 1.008000
27	opls_140	1	HDE	H14	27	0.1551 1.008000
28	opls_140	1	HDE	H15	28	0.1551 1.008000
29	opls_135	1	HDE	C9	29	-0.4965 12.011000
30	opls_140	1	HDE	H16	30	0.1591 1.008000
31	opls_140	1	HDE	H17	31	0.1591 1.008000
32	opls_140	1	HDE	H18	32	0.1591 1.008000
33	opls_137	1	HDE	C10	33	-0.1823 12.011000
34	opls_136	1	HDE	C11	34	-0.312 12.011000
35	opls_136	1	HDE	C12	35	-0.312 12.011000
36	opls_140	1	HDE	H19	36	0.1551 1.008000
37	opls_140	1	HDE	H20	37	0.1551 1.008000
38	opls_136	1	HDE	C13	38	-0.312 12.011000
39	opls_140	1	HDE	H21	39	0.1551 1.008000
40	opls_140	1	HDE	H22	40	0.1551 1.008000
41	opls_135	1	HDE	C14	41	-0.4965 12.011000
42	opls_140	1	HDE	H23	42	0.1551 1.008000
43	opls_140	1	HDE	H24	43	0.1551 1.008000
44	opls_136	1	HDE	C15	44	-0.312 12.011000
45	opls_140	1	HDE	H25	45	0.1591 1.008000
46	opls_140	1	HDE	H26	46	0.1591 1.008000
47	opls_140	1	HDE	H27	47	0.1591 1.008000
48	opls_140	1	HDE	H28	48	0.1551 1.008000
49	opls_140	1	HDE	H29	49	0.1551 1.008000
50	opls_135	1	HDE	C16	50	-0.4965 12.011000
51	opls_140	1	HDE	H30	51	0.1591 1.008000
52	opls_140	1	HDE	H31	52	0.1591 1.008000
53	opls_140	1	HDE	H32	53	0.1591 1.008000
54	opls_140	1	HDE	H33	54	0.1646 1.008000
55	opls_140	1	HDE	H34	55	0.1646 1.008000

[bonds]

1	2	1		
2	3	1		
2	4	1		
2	5	1		
4	6	1		
5	9	1		
6	7	1		
6	8	1		
6	33	1		

```

9 10 1
9 11 1
9 12 1
12 13 1
12 14 1
12 55 1
13 15 1
13 16 1
13 17 1
14 18 1
14 19 1
14 20 1
17 21 1
17 22 1
17 23 1
20 24 1
20 25 1
20 26 1
23 27 1
23 28 1
23 29 1
29 30 1
29 31 1
29 32 1
33 34 1
33 35 1
33 54 1
34 36 1
34 37 1
34 38 1
35 39 1
35 40 1
35 41 1
38 42 1
38 43 1
38 44 1
41 45 1
41 46 1
41 47 1
44 48 1
44 49 1
44 50 1
50 51 1
50 52 1
50 53 1
[ angles ]
1 2 3 1
1 2 4 1
1 2 5 1
3 2 4 1
3 2 5 1
4 2 5 1
2 4 6 1
2 5 9 1
4 6 7 1
4 6 8 1
4 6 33 1
7 6 8 1
7 6 33 1
8 6 33 1
5 9 10 1
5 9 11 1
5 9 12 1
10 9 11 1
10 9 12 1
11 9 12 1
9 12 13 1
9 12 14 1
9 12 55 1

```

13	12	14	1
13	12	55	1
14	12	55	1
12	13	15	1
12	13	16	1
12	13	17	1
15	13	16	1
15	13	17	1
16	13	17	1
12	14	18	1
12	14	19	1
12	14	20	1
18	14	19	1
18	14	20	1
19	14	20	1
13	17	21	1
13	17	22	1
13	17	23	1
21	17	22	1
21	17	23	1
22	17	23	1
14	20	24	1
14	20	25	1
14	20	26	1
24	20	25	1
24	20	26	1
25	20	26	1
17	23	27	1
17	23	28	1
17	23	29	1
27	23	28	1
27	23	29	1
28	23	29	1
23	29	30	1
23	29	31	1
23	29	32	1
30	29	31	1
30	29	32	1
31	29	32	1
6	33	34	1
6	33	35	1
6	33	54	1
34	33	35	1
34	33	54	1
35	33	54	1
33	34	36	1
33	34	37	1
33	34	38	1
36	34	37	1
36	34	38	1
37	34	38	1
33	35	39	1
33	35	40	1
33	35	41	1
39	35	40	1
39	35	41	1
40	35	41	1
34	38	42	1
34	38	43	1
34	38	44	1
42	38	43	1
42	38	44	1
43	38	44	1
35	41	45	1
35	41	46	1
35	41	47	1
45	41	46	1
45	41	47	1
46	41	47	1

38	44	48	1
38	44	49	1
38	44	50	1
48	44	49	1
48	44	50	1
49	44	50	1
44	50	51	1
44	50	52	1
44	50	53	1
51	50	52	1
51	50	53	1
52	50	53	1
[dihedrals]			
1	2	4	6
3	2	4	6
5	2	4	6
1	2	5	9
3	2	5	9
4	2	5	9
2	4	6	7
2	4	6	8
2	4	6	33
2	5	9	10
2	5	9	11
2	5	9	12
4	6	33	34
4	6	33	35
4	6	33	54
7	6	33	34
7	6	33	35
7	6	33	54
8	6	33	34
8	6	33	35
8	6	33	54
5	9	12	13
5	9	12	14
5	9	12	55
10	9	12	13
10	9	12	14
10	9	12	55
11	9	12	13
11	9	12	14
11	9	12	55
9	12	13	15
9	12	13	16
9	12	13	17
14	12	13	15
14	12	13	16
14	12	13	17
55	12	13	15
55	12	13	16
55	12	13	17
9	12	14	18
9	12	14	19
9	12	14	20
13	12	14	18
13	12	14	19
13	12	14	20
55	12	14	18
55	12	14	19
55	12	14	20
12	13	17	21
12	13	17	22
12	13	17	23
15	13	17	21
15	13	17	22
15	13	17	23
16	13	17	21
16	13	17	22

16	13	17	23	3
12	14	20	24	3
12	14	20	25	3
12	14	20	26	3
18	14	20	24	3
18	14	20	25	3
18	14	20	26	3
19	14	20	24	3
19	14	20	25	3
19	14	20	26	3
13	17	23	27	3
13	17	23	28	3
13	17	23	29	3
21	17	23	27	3
21	17	23	28	3
21	17	23	29	3
22	17	23	27	3
22	17	23	28	3
22	17	23	29	3
17	23	29	30	3
17	23	29	31	3
17	23	29	32	3
27	23	29	30	3
27	23	29	31	3
27	23	29	32	3
28	23	29	30	3
28	23	29	31	3
28	23	29	32	3
6	33	34	36	3
6	33	34	37	3
6	33	34	38	3
35	33	34	36	3
35	33	34	37	3
35	33	34	38	3
54	33	34	36	3
54	33	34	37	3
54	33	34	38	3
6	33	35	39	3
6	33	35	40	3
6	33	35	41	3
34	33	35	39	3
34	33	35	40	3
34	33	35	41	3
54	33	35	39	3
54	33	35	40	3
54	33	35	41	3
33	34	38	42	3
33	34	38	43	3
33	34	38	44	3
36	34	38	42	3
36	34	38	43	3
36	34	38	44	3
37	34	38	42	3
37	34	38	43	3
37	34	38	44	3
33	35	41	45	3
33	35	41	46	3
33	35	41	47	3
39	35	41	45	3
39	35	41	46	3
39	35	41	47	3
40	35	41	45	3
40	35	41	46	3
40	35	41	47	3
34	38	44	48	3
34	38	44	49	3
34	38	44	50	3
42	38	44	48	3
42	38	44	49	3

```

42 38 44 50 3
43 38 44 48 3
43 38 44 49 3
43 38 44 50 3
38 44 50 51 3
38 44 50 52 3
38 44 50 53 3
48 44 50 51 3
48 44 50 52 3
48 44 50 53 3
49 44 50 51 3
49 44 50 52 3
49 44 50 53 3
[ pairs ]
1 6
1 9
2 7
2 8
2 10
2 11
2 12
2 33
3 6
3 9
4 9
4 34
4 35
4 54
5 6
5 13
5 14
5 55
6 36
6 37
6 38
6 39
6 40
6 41
7 34
7 35
7 54
8 34
8 35
8 54
9 15
9 16
9 17
9 18
9 19
9 20
10 13
10 14
10 55
11 13
11 14
11 55
12 21
12 22
12 23
12 24
12 25
12 26
13 18
13 19
13 20
13 27
13 28
13 29
14 15

```

14	16
14	17
15	21
15	22
15	23
15	55
16	21
16	22
16	23
16	55
17	30
17	31
17	32
17	55
18	24
18	25
18	26
18	55
19	24
19	25
19	26
19	55
20	55
21	27
21	28
21	29
22	27
22	28
22	29
27	30
27	31
27	32
28	30
28	31
28	32
33	42
33	43
33	44
33	45
33	46
33	47
34	39
34	40
34	41
34	48
34	49
34	50
35	36
35	37
35	38
36	42
36	43
36	44
36	54
37	42
37	43
37	44
37	54
38	51
38	52
38	53
38	54
39	45
39	46
39	47
39	54
40	45
40	46
40	47

40 54
41 54
42 48
42 49
42 50
43 48
43 49
43 50
48 51
48 52
48 53
49 51
49 52
49 53